

## Extending the supercontinuum spectrum down to 200 nm with few-cycle pulses

N Aközbek<sup>1</sup>, S A Trushin<sup>2</sup>, A Baltuška<sup>2</sup>, W Fuß<sup>2,5</sup>,  
E Goulielmakis<sup>2</sup>, K Kosma<sup>2</sup>, F Krausz<sup>2</sup>, S Panja<sup>2</sup>,  
M Uiberacker<sup>2</sup>, W E Schmid<sup>2</sup>, A Becker<sup>3</sup>, M Scalora<sup>4</sup>  
and M Bloemer<sup>4</sup>

<sup>1</sup> Time Domain Corporation, 7057 Old Madison Pike, Huntsville,  
AL 35806, USA

<sup>2</sup> Max-Planck-Institut für Quantenoptik, D-85748 Garching, Germany

<sup>3</sup> Max-Planck Institut für Physik Komplexer Systeme, Nöthnitzer Str.,  
D-01187 Dresden, Germany

<sup>4</sup> Charles M. Bowden Research Center, Research Development and Engineering  
Center, Redstone Arsenal, AL 35898, USA

E-mail: [neset.akozbek@timedomain.com](mailto:neset.akozbek@timedomain.com) and [w.fuss@mpq.mpg.de](mailto:w.fuss@mpq.mpg.de)

*New Journal of Physics* **8** (2006) 177

Received 26 May 2006

Published 5 September 2006

Online at <http://www.njp.org/>

doi:10.1088/1367-2630/8/9/177

**Abstract.** By focusing 805 nm pulses of low energy (0.2–1 mJ) into atmospheric-pressure argon, a supercontinuum is generated with a short-wavelength cutoff of 640, 250 and 210 nm for initial pulse durations of 45, 10 and 6 fs, respectively. It is shown numerically that the large shift of the UV cutoff and many features of the spectrum are caused by terms beyond the slowly-varying-envelope approximation (SVEA). Their effect on pulse compression and filament length is also discussed.

<sup>5</sup> Author to whom any correspondence should be addressed.

**Contents**

<b>1. Introduction</b>	<b>2</b>
<b>2. Experimental method and results</b>	<b>3</b>
<b>3. Theoretical results and discussion</b>	<b>4</b>
<b>4. Conclusion</b>	<b>10</b>
<b>Acknowledgments</b>	<b>10</b>
<b>References</b>	<b>10</b>

**1. Introduction**

Supercontinuum generation is a phenomenon first observed 36 years ago [1] and since then has been widely studied in various optical media including gases, condensed matter and engineered microstructures such as photonic crystal fibres [2, 3]. Some of the latest developments can be found in a special issue on continuum generation in [3], and recent reviews on self-focusing and filamentation of femtosecond pulses are available [4, 5]. Spectral broadening, generating the continuum, is in general described by self-phase modulation [6]. In bulk media, there is a certain power threshold above which continuum generation is initiated, which in general coincides with the threshold of self-focusing [2]. Furthermore, it has been shown that in solid media there is a band-gap energy threshold, below which no continuum generation is observed [7]. In addition to self-phase modulation, other effects such as self-steepening and space-time focusing [8] may become important. Therefore, the physical mechanisms that contribute to continuum generation can be complex. An important feature of continuum generation is the UV cutoff wavelength. It seems to be limited by a number of effects such as intensity clamping and plasma generation [9], as well as linear chromatic dispersion [10]. However, using long pulses (50–150 fs) and high powers it was recently shown that a third harmonic is generated in air, which undergoes spectral broadening due to cross phase modulation [11]–[13]. It was suggested in these studies that the UV cutoff of the continuum spectra can thereby be further extended into the UV, when the broadened spectra of the fundamental and third harmonic in air [12, 13] and of higher-order harmonics in argon [14, 15] merge together. We show below that with few-cycle pulses, harmonics are not required to explain the observed spectra.

Recently we demonstrated that focusing of 10 fs Ti-sapphire laser pulses of moderate energy ( $\leq 0.3$  mJ) into atmospheric-pressure argon (focal length 1 m) produces collimated radiation with a continuous spectrum (supercontinuum) extending down to 250 nm [16]. The radiation is produced under conditions where self-focusing and filamentation occur. Increasing the pulse energy to slightly above 0.35 mJ caused a breakdown into multiple filaments and a shift of the UV cutoff to longer wavelengths. With longer pulses (50–150 fs), UV cutoffs of similar or even shorter wavelengths have only been obtained with 10–100 times higher powers under conditions of multiple filamentation in air and other gases [13]–[15]. In addition, much longer interaction lengths are required in these cases. Clearly, ultrashort pulse durations down to a few cycles are the reason that only moderate powers were needed in our study [16]. In a simple theory based on self-phase modulation by the optical Kerr effect only, the total frequency spread  $\Delta\omega$  of the supercontinuum is predicted to be  $\Delta\omega \propto \tau_p^{-1}z$ , that is, proportional to the inverse pulse duration and the interaction length at high intensity [17]. To check how far the cutoff can actually be

pushed into the UV, we measured supercontinuum spectra using pulses of  $\tau_p = 45$  fs down to 6 fs and different interaction lengths  $z$ . A simple proportionality to  $\tau_p^{-1}z$  is not confirmed and in principle cannot be expected, because continuum generation in the case of few-cycle pulses involves effects beyond a simple self-phase modulation model. Hence, we use a model that includes higher-order terms such as self-steepening and show that many features of the observed spectra can be reproduced. The experimental results thus provide a simple test case for the model. In contrast to previous studies, complications such as multiple filamentation, averaging over many pulses or molecular effects such as stimulated Raman scattering are avoided in our experiment.

The supercontinuum produced by the short pulses not only provides a large bandwidth for spectroscopy, but might also be an attractive and rugged source of short or compressible pulses tunable over such a wide wavelength range. In fact, the range near 800 nm has been further compressed in Zürich to 5.1 fs [18]. However, valence excitation of molecules usually requires wavelengths in the UV spectral region. The supercontinuum is broad enough that pulses in this region with near 1 fs duration could be calculated in the transform limit (which would require a smooth spectral phase). Sub-femtosecond pulses in the soft x-ray region, suitable for probing after such an excitation, are already available [19]. On the other hand, our first attempt at pulse compression using radiation cut out near the UV cutoff reached a pulse duration of 70 fs, which is still far from the transform limit [16]. It would therefore be desirable to understand in more detail the properties of this radiation, in particular near the UV cutoff, and how it depends on the initial laser pulse parameters. The model calculations presented here also serve this purpose.

## 2. Experimental method and results

The experimental method is described in [16]. Briefly, we focused up to 1 mJ of the 45 fs pulses of a commercial Ti-sapphire laser system (800 nm) by an  $f = 2$  m concave mirror into a windowless first glass cell (length 1.5 m) with slowly flowing argon at ambient pressure (950 mbar). After recollimation and reflection from chirped mirrors, the pulses had a duration of 10 fs. By a variable diaphragm they were reduced in diameter ( $\leq 5$  mm) and energy ( $\leq 0.35$  mJ) and then refocused ( $f = 1$  m) into a second such cell. The emerging radiation was integrated over its cross-section before analysis took place in a spectrograph. The resulting spectrum ‘10 fs, 0.35 mJ’ is shown in figure 1(a). The spectrum ‘45 fs, 1 mJ’ in this figure was obtained in the same setup by skipping the first cell and the chirped mirrors. The results with the pulse length  $\tau_p = 6$  fs and energy 0.2 mJ were obtained by focusing pulses of this duration (from the laser system LWS01 at Garching, described in [20]) into the second cell. The two shorter pulses have the same peak power (33–35 GW) and the longer one is slightly weaker (22 GW).

It is obvious from figure 1(a) that the shorter the pulses, the farther in the UV is the cutoff. It is pushed from 250 to 210 nm in going from 10 to 6 fs. This displacement is much smaller than for the pair 45/10 fs. It is also smaller than a frequency extension  $\Delta\omega$  proportional to  $\tau_p^{-1}$ , that was suggested in [16] (see also [17]). This expectation was based on the idea that Kerr-effect self-phase modulation contains the derivative of the intensity  $I$  and that the maximum  $dI/dt \propto \tau_p^{-1}$ . However, in such a simple model ignoring higher-order terms and propagation effects, the shifts of the phase and frequency should also be  $\propto z$ , the interaction length at high intensity [16, 17]. We found that the length  $z_f$  of the luminescing filament was indeed shorter with the shortest pulses, as roughly judged by inspection:  $z_f = 8$ –10, 12 and 7.5 cm for  $\tau_p = 45$ , 10

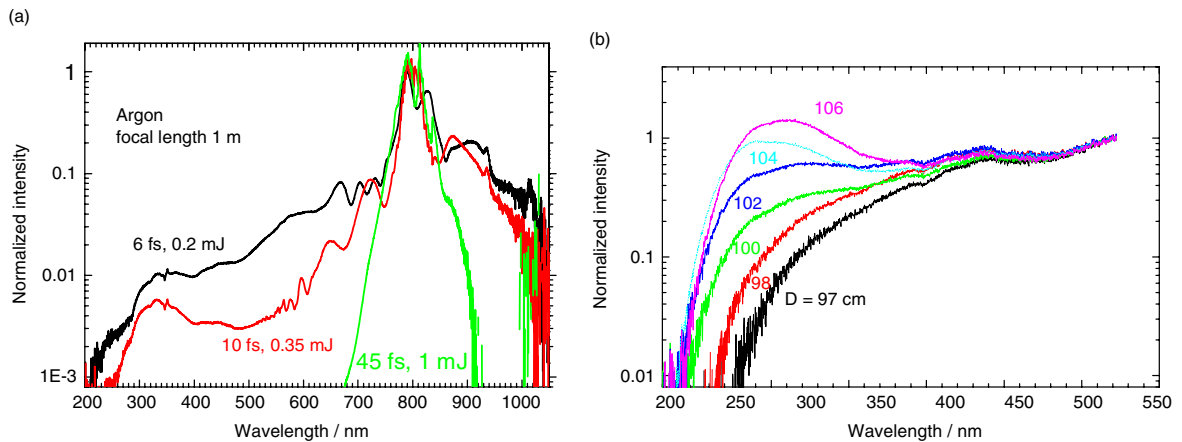


**Figure 1.** (a) Spectra measured with different pulse durations by a broad-band spectrometer. (b) Spectra measured by a UV spectrometer with  $\tau_p = 10$  fs, terminating filamentation at different distances  $D$  from the focusing mirror (the starting point for the calculations,  $z = 0$ , is at about  $D = 92$  cm). The spectra in (a) are normalized at 800 nm, those in (b) at 520 nm. In (a), the feature with maximum at 350 and minimum at 344 nm is an artefact of the broad-band spectrometer.

and 6 fs, respectively; the reduced  $z_f$  can thus partially compensate the larger shift by pulse shortening. The present calculation not only reproduces the spectra but also the change of the filament length (see below).

Figure 1(b) shows the effect of controlling the filament length  $z_f$ , using the 10 fs pulses. This length was varied by terminating filamentation by a pinhole of diameter  $150 \mu\text{m}$ , placed in the focal region at various distances  $D$  from the focusing mirror [16]; the effect is based on eliminating the background reservoir (lower-intensity regions of the beam profile [21]–[23]) by the pinhole [4, 24]. It can be seen that increasing  $D$  (increasing  $z_f$ ) in fact initially shifts the cutoff to shorter wavelengths. But the last centimetres only give rise to an intensity increase around 300–330 nm. (The maximum at 320 nm can also be recognized in figure 1(a) in the 10 fs spectrum.) This is also found in the calculations (see below).

We also checked whether the carrier-envelope phase of the 6 fs pulses has any effect on the spectrum. But the spectra were indistinguishable, whether sine or cosine pulses were employed. Hence the carrier-envelope phase does not play a significant role in the generation of the supercontinuum.

### 3. Theoretical results and discussion

In order to get insight into the various nonlinear contributions to the continuum generation, we calculate numerically the propagation of the electric field  $E(r, z, t) = A(r, z, t)e^{-i\omega_0 t + ikz} + \text{c.c.}$ , where  $A(r, z, t)$  is an envelope function (normalized so that  $|A|^2$  is the intensity). Here, we adapt a propagation equation (equation (1)) for  $A$ , that reaches beyond the slowly-varying-envelope approximation (SVEA). It was introduced by Brabec and Krausz [25, 26] and is referred to as the slowly-evolving-wave approximation. It was shown to be valid even for one-cycle pulses, if the

difference of group and phase velocities is small enough [25]. Here, the underlying envelope propagation equation is written in the retarded coordinate frame ( $\tau = t - z/v_g$ ) as in [27].

$$\left( i \frac{\partial}{\partial z} + \frac{1}{2k} T^{-1} \nabla_{\perp}^2 - \frac{k''}{2} \frac{\partial^2}{\partial \tau^2} - i \frac{k'''}{6} \frac{\partial^3}{\partial \tau^3} + T n_2 k_0 |A|^2 - \frac{e^2}{2\epsilon_0 k m_e c^2} N_e \right) A(r, z, \tau) = 0 \quad (1)$$

This equation contains higher-order terms going beyond the SVEA in the form of the operator  $T = \left( 1 + i \frac{1}{\omega_0} \frac{\partial}{\partial \tau} \right)$ . The SVEA is recovered by setting  $T = 1$ . The derivative terms in  $T$  are expected to become more important with shorter pulses (initial duration  $\tau_p$ ), in particular if the number of cycles per pulse ( $= \omega_0 \tau_p / 2\pi$ ) is small. These terms are responsible for effects such as self-steepening and space-time focusing [8], [25]–[27].

As compared to [27], we have neglected any time dependence of the nonlinear refractive index  $n_2$  (which would be caused by the Raman effect in molecular gases). However, equation (1) includes all the main linear and nonlinear effects such as self-focusing, diffraction, plasma generation, group-velocity dispersion, and self-steepening. Plasma (electron density  $N_e$ ) generation is calculated by

$$\frac{\partial N_e}{\partial \tau} = (N_0 - N_e) \sigma^{(n)} |A|^{2n}, \quad (2)$$

where  $N_0$  is the neutral gas density. The ionization rate is fitted by a power law of the form  $\sigma^{(n)} I^n$  with  $\sigma^{(n)} = 1.93 \times 10^{-104} \text{ s}^{-1} (\text{cm}^2 \text{ W}^{-1})^n$  and  $n = 8.22$  as in [28]. For the nonlinear index of Ar, we used  $n_2 = 1.4 \times 10^{-19} \text{ cm}^2 \text{ W}^{-1}$  [29]. A convenient parameter is the critical power for self-focusing  $P_{\text{cr}}$ , for which we use  $P_{\text{cr}} = \lambda^2 / 2\pi n_2 = 7.3 \text{ GW}$  ( $\lambda = 800 \text{ nm}$ ). Both second- and third-order group velocity dispersion (with coefficients  $k'' = 0.2 \text{ fs}^2 \text{ cm}^{-1}$  and  $k''' = 0.1 \text{ fs}^3 \text{ cm}^{-1}$ ) are included in equation (1). Group velocity dispersion is not negligible in the current case, even though the nonlinear interaction length (filament length  $\approx 10 \text{ cm}$ ) is clearly shorter than the dispersion length ( $L_{\text{dis}} = \tau_p^2 / (4 \ln 2 k'') = 180 \text{ cm}$  for an initial pulse duration of  $\tau_p = 10 \text{ fs}$ ).

The numerical simulations were carried out using input conditions close to those of the experiment. Since up to the self-focusing distance, the propagation could mainly be described by linear effects, the input field for the calculations was taken as a collimated beam with a beam radius of 0.2 mm, which is taken as starting point ( $z = 0$ ) for the propagation. This point is at a distance from the focusing mirror of  $D \approx 92 \text{ cm}$ . Different values of the critical power  $P_{\text{cr}}$  and the power itself  $P_0$  were tried out. With  $P_{\text{cr}} = 7.3 \text{ GW}$ , which is based on the published [29]  $n_2$  value (see above) and  $P_0 = 3P_{\text{cr}}$ , we obtain the best agreement with the experiment for the cutoff wavelength and the position of the maximum near 300 nm.

Figure 2 shows spectra for the three pulse durations, calculated at different propagation distances  $z$ , integrated over the beam cross-section. In particular in the short-wavelength part, the spectra and their dependence on  $\tau_p$  and  $z$  are very well reproduced. (See below for the region near 800 nm.) The cutoff is strongly pushed to the UV on going from 45 to 10 fs and only a little more on reducing the pulse duration to 6 fs, just as in the experiment. Even the absolute values of the cutoff wavelengths agree with the experiment. Also the shapes of the spectra fit well: on increasing the pathlength  $z$  with the 10 fs pulses (figure 2(c)), the cutoff is not much shifted between  $z = 10$  and 15 cm (to be discussed below); instead, the intensity around 320 nm increases, eventually giving rise to a maximum. With 6 fs, there is no clearly developed maximum in this region. Obviously, the model calculations recapture most of the experimentally observed

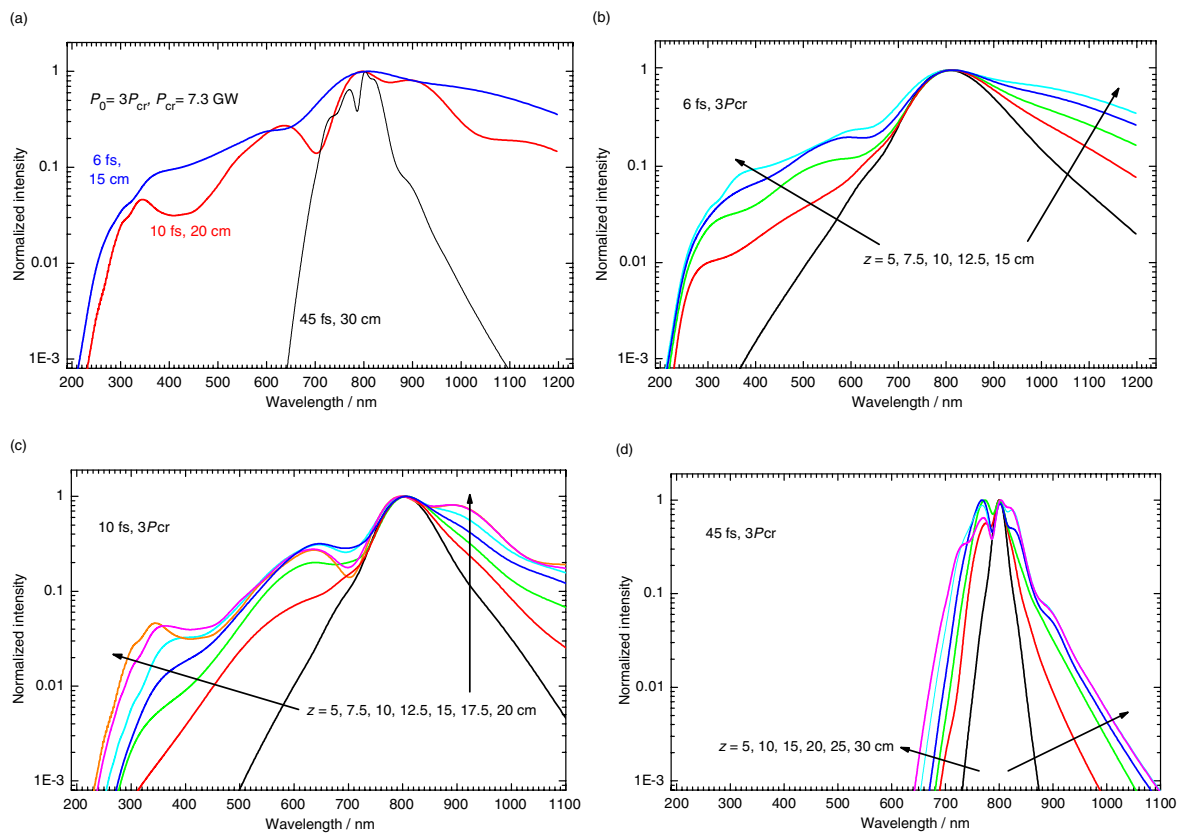


**Figure 2.** (a) Spectra calculated for different pulse durations. (b) Spectra calculated for 6 fs at different  $z$ . (c) Spectra calculated for 10 fs at different  $z$ . (d) Spectra calculated for 45 fs at different  $z$ .

spectral features in the UV and we obtain a more than qualitative agreement between theory and experiment.

The calculated halfwidths ( $\geq 100$  nm with 10 fs, for instance; figure 2) near 800 nm are larger than observed (50–100 nm; figure 1). Also the maxima in this region, relative to the UV part, are lower in the calculation. We believe that this difference is caused by low-intensity spatial (and temporal) wings of the beam, deviating from a Gaussian profile. In fact in [16], a red (800 nm) outer ring was observed, probably caused by diffraction at the input diaphragm. Due to its low intensity, it is not expected to be greatly broadened, so that it contributes a narrow-halfwidth component to the spatially integrated spectrum. Another minor deviation concerns the modulations that are seen in the spectrum in particular between 800 and 500 nm. They have a coarser structure in the calculations (figure 2) than in the experiments (figure 1). However, they are believed to result from interferences depending only on fine details of the propagation of the radiation [17], which do not carry much information.

It is worth mentioning that the calculations were done for a single laser pulse. In the measurements, the spectra were averaged over 2 to about 10000 pulses, the latter only with the broad-band spectrometer (which has low sensitivity in the UV) in the region of the UV cutoff. In the high-intensity region of the spectra of figure 1(a) (broad-band spectrometer) and in the spectra with the UV spectrometer (figure 1(b)), where comparison is possible, no difference



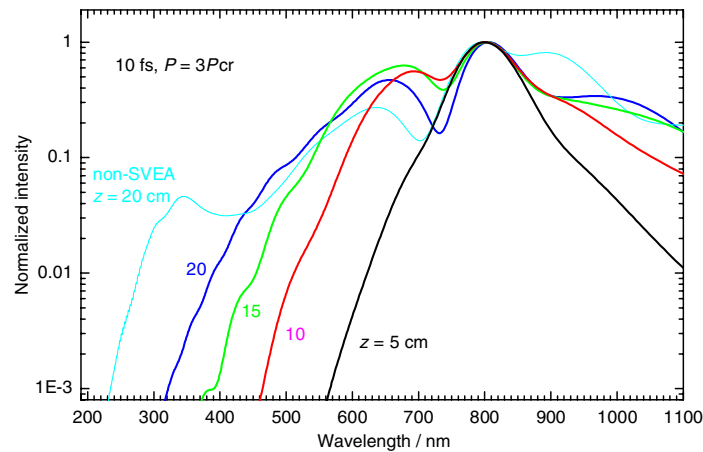


**Figure 3.** SVEA spectra calculated for 10 fs at different  $z$ . The thinner line shows for comparison the non-SVEA spectrum at  $z = 20$  cm from figure 2(a).

could be recognized between different degrees of averaging. In particular, fine spectral features such as the modulations are fully reproducible. This is in contrast to previous experiments under conditions of multiple filamentation, where large pulse-to-pulse variations of the spectra were observed (e.g. in [14]) and smooth spectra were only obtained by averaging.

It is also worth noting that the good agreement in the UV (obtained for the few-cycle pulses) is obtained without taking any third-harmonic generation into account. Previous observations of such broad continua (at higher powers in air with longer pulses) invoked co-propagation of the third harmonic with the fundamental, its broadening by cross-phase modulation and eventual merging with the longer-wavelength continuum [11]–[13]. Moreover, this process could be noncritically phase matched, and the third-harmonic frequency can be shifted [30]. However, in our experiment with few-cycle pulses and relatively weak power and a single filament with long paths in Ar, a third harmonic was weaker by at least two orders of magnitude than the supercontinuum (Trushin *et al.*, to be published).

Continuum generation usually involves many effects, and in some cases it is difficult to isolate the individual contributions. To obtain further physical insight, we compare the spectral broadening in the framework of the usual SVEA with the non-SVEA propagation models. In the former, we omitted from equation (1) the non-SVEA term by setting  $T = 1$ . The comparison is shown in figure 3.

Obviously the SVEA model gives rise to much less broadening than observed, the cutoff is steadily blue-shifted in contrast to the experiment, and the calculated spectra do not have much similarity with the UV part of the measured spectrum. (The halfwidth is practically unaffected by the non-SVEA terms.) This is in contrast to the non-SVEA calculations (figure 2(c)), which reproduce the broadening and every spectral feature in the UV. These features can therefore be considered as a clear signature of the crucial role of the non-SVEA terms for the propagation of few-cycle pulses, at least for the current set of parameters. This also gives credibility to the calculated pulse shapes (see below), which are shortened by self-steepening due to the non-SVEA terms. These results are also in good agreement with the calculations of Gaeta [8] who was the first to show that even with longer pulses (100 cycles) self-steepening and space-time focusing effects are important, which causes the steepening of the trailing edge of the pulse, resulting in a broad blue-shifted pedestal spectrum (see also [27]).

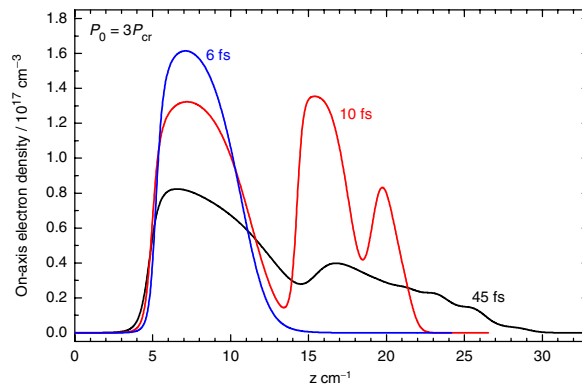


**Figure 4.** Calculated on-axis electron density for different pulses.

The filaments terminate not only in the experiment but also in the calculation. This can already be inferred from the fact that on the last few centimetres of  $z$ , there is only little change of the spectra (figure 2). The filament lengths can, however, be better recognized in a plot of the on-axis electron density. This is shown in figure 4.

The calculated lengths are similar to the observed ones. They shrink with the pulse durations. The second maximum for the two longer pulses is obviously caused by refocusing [23], which has often been observed in laser pulse filamentation (see, e.g. [2]). This refocusing seems not to work with the shortest pulses. Comparison with figure 2(c) shows that the last shift of the UV cutoff occurs just at the refocusing distance. It may also be worth noting in figure 4 that the shorter pulses give rise to slightly higher electron densities; they are connected with slightly higher intensities (not shown).

Self-focusing normally leads to self-guiding, in which Kerr-effect focusing is balanced by defocusing caused by the plasma near the axis (see e.g. the review [4]). It is therefore not obvious why the filament should terminate. It has been suggested that losses by ionization or conical emission could be the cause [31]. But this mechanism can only apply for filaments, that are much longer (e.g. tens of metres) than ours, because the power would have to be reduced by a factor of 3–4, to below the critical power; losses were not measurable in our case [16]. The observation that filaments often terminate at a distance near the diffraction length (consistent with our observations [16]) has been rationalized with the moving-focus model [22]; but this model depends on the SVEA. Furthermore, much longer propagation lengths have also been observed [32]. Very recently, diffraction by the plasma was suggested to terminate the filaments [33]. (In previous experiments with longer pulses, the shorter wavelengths were in cones of larger opening angles; see, e.g., the review [4]. By contrast, with the 10 fs pulses used in our experiment conical emission was not noticeable [16]: The shortest wavelengths were on the axis, and it is worth noting that also this property is reproduced by the calculations. Indeed this has been predicted by Brabec and Krausz [25], who pointed to the inverse non-SVEA operator  $T^{-1}$  in front of the diffraction term: it increases the divergence of the low-frequency components of the spectrum.) Because losses by ionization or conical emission were negligible, we supposed in [16] that the pulses are lengthened in the filament by a factor, so that the power is lowered to below  $P_{cr}$ . Indeed, the calculation confirms this conjecture: figure 5 shows the calculated on-axis temporal intensity profiles with the different initial pulse durations.



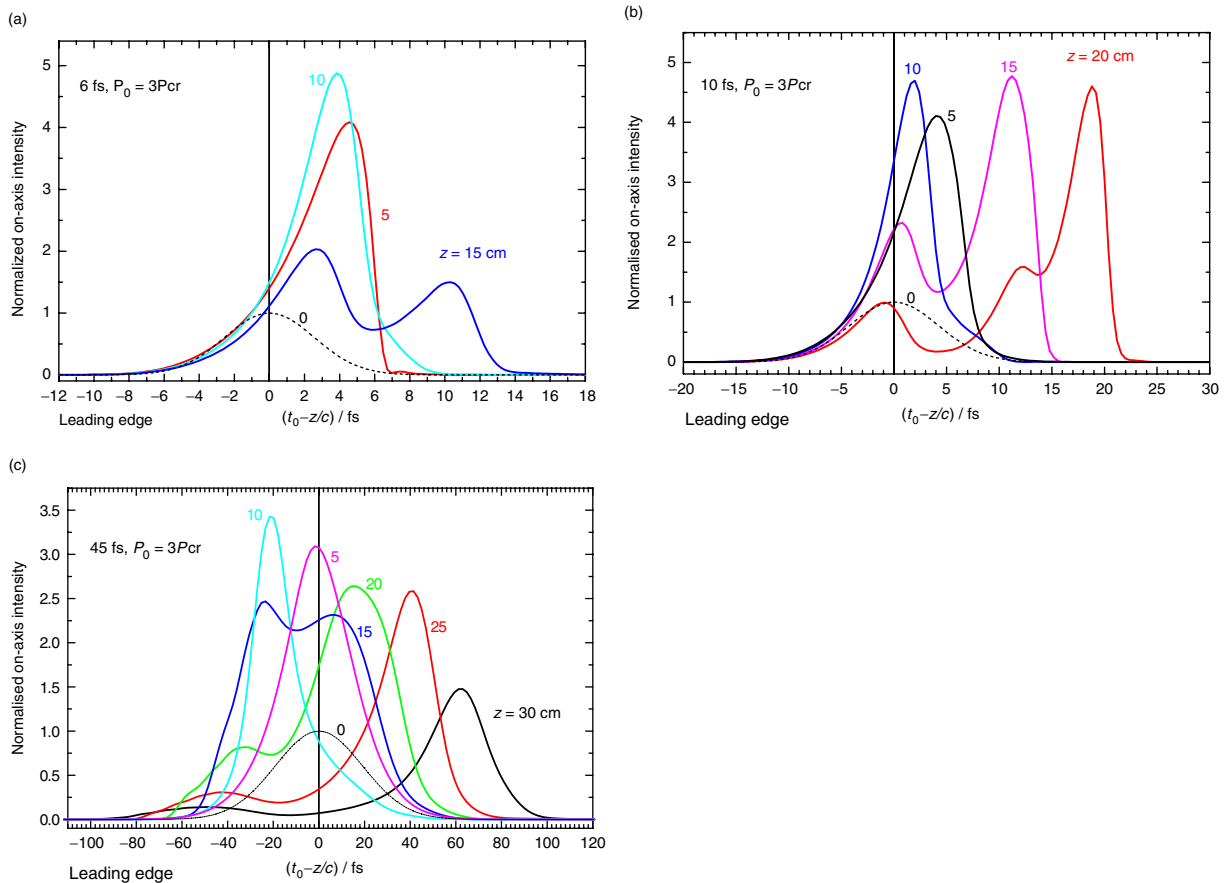


**Figure 5.** Calculated normalized on-axis intensity for different initial pulse durations at different  $z$ : (a) 6 fs; (b) 10 fs; (c) 45 fs.

Initially the intensity on the axis grows by a factor of 3–5 due to self-focusing. Then, after sufficiently long propagation ( $z > 10$  cm), the pulses are split and thus become longer. This is especially well evidenced for the case of 6 fs (figure 5(a)). At the end of the filament ( $z = 15$  cm), the pulse is lengthened by factor of 2 to  $\approx 12$  fs. For the 10-fs case, the splitting occurs just where the electron density (figure 4) indicates a refocusing. This lengthening is likely to also reduce the power (i.e., the intensity integrated over the cross-section) to near  $P_{\text{cr}}$ , so that the filament is prone to terminate. The calculation also reveals that inclusion of the non-SVEA (T) and the dispersion ( $k''$  and  $k'''$ ) terms in equation (1) both shorten the filaments (not shown).

On the other hand, the 10 and 6 fs pulses are initially (at  $z = 10$  cm) *shortened* to 5.5 and 4.5 fs. This is brought about by steepening of the trailing edge, caused by a slower travelling of the peak compared with the rest of the pulse (already due to the  $n_2 I$  term, see, e.g., [4]), and by steepening of the leading edge due to the non-SVEA terms. It is remarkable that even the shorter pulses, which contain only a few cycles, are temporarily steepened and shortened. (It is worth noting that the calculations obviously work even for few-cycle pulses, as indicated by the agreement with the measured spectrum.) Figure 5 suggests, however, that the self-shortening of the pulses could be exploited, if the filament is artificially terminated (at distances close to the centre of the first focus at  $z \leq 10$  cm). A method to do so would use cutting off the spatial background reservoir by a pinhole as in figure 1(b). A recent work suggested instead to generate

a filament in a pressure gradient [34]. Another recent calculation predicted a pulse shortening only after (instead of before, as in our study) a pulse splitting [35]. The latter work describes the propagation by an equation where the time dependence has been transformed to the frequency domain; it also contains self-steepening terms. These terms could be checked by the spectral features in the UV (which are easier to measure than the pulse shapes). Previous observation of pulse self-compression, starting from longer pulses, invoked a higher-order refractive index ( $n_4$ ) [36]. (For other influences on pulse shortening also in condensed media, see [37] and literature quoted there.)

From a practical point of view, it is important to know whether such short pulse durations are also feasible all over the spectral region of this supercontinuum. The spectral phase dependence was not investigated. However, the fact, that the whole pulse splitting can increase the pulse duration at the end of the filament by not more than a factor of two, gives an upper limit. In full agreement with this limit, we were recently able to compress a spectral cut (halfwidth 9 nm) from the supercontinuum at 280 nm to about 30 fs, which is only twice as long as the pump pulse [38]. However, it is not clear whether this pulse duration is limited by intrinsic properties of the supercontinuum or by the prism compressor.

#### 4. Conclusion

We demonstrated experimentally and theoretically that already by focusing pulses of moderate powers into argon—under conditions of self-focusing with only a single filament—a supercontinuum is produced, whose UV cutoff is pushed to shorter wavelengths the shorter the pulses, reaching 210 nm starting with 6 fs. (A preliminary calculation indicates that with 4 fs pulses, one could extend the spectrum far into the vacuum UV.) The calculations reproduce the observed spectra in the UV in all details. They also find that the filaments are shorter with shorter pulses, as observed. The filaments terminate due to group-velocity dispersion (although the dispersion lengths are much longer than the filaments) and non-SVEA terms. The calculations do not involve production (and co-propagation) of any third harmonic; its contribution to the spectra seems negligible, if one starts with few-cycle pulses. It was shown that non-SVEA terms also play a crucial role for the continuum spectra generated by few-cycle pulses. The spectral features near the UV cutoff can even be considered as a clear signature of these terms. They also cause self-compression of the pulses. To exploit this shortening, one should, however, limit the length of the filaments. It must still be investigated whether such short pulse durations are also feasible all over the spectral region of this supercontinuum.

#### Acknowledgments

This work was supported by the Deutsche Forschungsgemeinschaft (project FU 363/1) and the European Union's Human Potential Program under contract MRTN-CT-2003-505138 (XTRA).

#### References

- [1] Alfano R R and Shapiro S L 1970 *Phys. Rev. Lett.* **24** 584–7
- [2] Alfano R R 1989 *The Supercontinuum Laser Source* (New York: Springer)
- [3] Zheltikov A 2003 *Appl. Phys. B* **77** 143–59 (special issue on supercontinuum generation)

- [4] Chin S L *et al* 2005 *Can. J. Phys.* **83** 863–905
- [5] Kandidov V P, Kosareva O G, Golubtsov I S, Liu W, Becker A, Aközbebek N, Bowden C M and Chin S L 2003 *Appl. Phys. B* **77** 149–65
- [6] Agrawal G P 1995 *Nonlinear Fiber Optics* (San Diego, CA: Academic)
- [7] Brodeur A and Chin S L 1998 *Phys. Rev. Lett.* **80** 4406–9  
Brodeur A and Chin S L 1999 *J. Opt. Soc. Am. B* **16** 637–50
- [8] Gaeta A L 2000 *Phys. Rev. Lett.* **84** 3582–5
- [9] Liu W, Petit S, Becker A, Aközbebek N, Bowden C M and Chin S L 2002 *Opt. Commun.* **202** 189–97  
Becker A, Aközbebek N, Vijayalakshmi K, Oral E, Bowden C M and Chin S L 2001 *Appl. Phys. B* **73** 287–90
- [10] Kolesik M, Katona G, Moloney J V and Wright E M 2003 *Phys. Rev. Lett.* **91** 043905
- [11] Aközbebek N, Iwasaki A, Becker A, Scalora M, Chin S L and Bowden C M 2002 *Phys. Rev. Lett.* **89** 143901  
Yang H *et al* 2003 *Phys. Rev. E* **67** 015401 (R)  
Théberge F, Aközbebek N, Liu W, Gravel J F and Chin S L 2005 *Opt. Commun.* **245** 399–405  
Alexeev I, Ting A C, Gordon D F, Briscoe E, Hafizi B and Sprangle P 2005 *Opt. Lett.* **30** 1503–5  
Théberge F, Liu W, Hosseini S A, Luo Q, Sharifi S M and Chin S L 2005 *Appl. Phys. B* **81** 131–4  
Théberge F, Luo Q, Liu W, Hosseini S A, Sharifi S M and Chin S L 2005 *Appl. Phys. Lett.* **87** 081108
- [12] Aközbebek N, Becker A, Scalora M, Chin S L and Bowden C M 2003 *Appl. Phys. B* **77** 177–83
- [13] Théberge F, Liu W, Luo Q and Chin S L 2005 *Appl. Phys. B* **80** 221–5  
Bergé L, Skupin S, Méjean G, Kasparian J, Yu J, Frey S, Salmon E and Wolf J P 2005 *Phys. Rev. E* **71** 016602  
Méjean G, Kasparian J, Yu J, Frey S, Salmon E, Ackerman R, Wolf J P, Bergé L and Skupin S 2006 *Appl. Phys. B* **82** 341–5
- [14] Nishioka H, Odajima W, Ueda K and Takuma H 1995 *Opt. Lett.* **20** 2505–7
- [15] Nishioka H and Ueda K 2003 *Appl. Phys. B* **77** 171–5
- [16] Trushin S A, Panja S, Kosma K, Schmid W E and Fuß W 2005 *Appl. Phys. B* **80** 399–403
- [17] Manassah J T 1989 Simple models of self-phase and induced phase modulation *The Supercontinuum Laser Source* ed R R Alfano (New York: Springer)
- [18] Hauri C P, Kornelis W, Helbing F W, Heinrich A, Couairon A, Mysyrowicz A, Biegert J and Keller U 2004 *Appl. Phys. B* **79** 673–7  
Hauri C P, Guandalini A, Eckle P, Kornelis W, Biegert J and Keller U 2005 *Opt. Express* **13** 7541–7
- [19] Hentschel M, Kienberger R, Spielberger C, Reider G A, Milosevic N, Brabec T, Corkum P B, Heinzmann U and Drescher M 2001 *Nature* **414** 509–13  
Baltuška A *et al* 2003 *Nature* **42** 611–5  
Kienberger R *et al* 2004 *Nature* **427** 817–21
- [20] Kienberger R, Hentschel M, Spielmann C, Reider G A, Milosevic N, Heinzmann U, Drescher M and Krausz F 2002 *Appl. Phys. B* **74** S3–9
- [21] Nibbering E T J, Curley P F, Grillon G, Prade B S, Franco M A, Salin F and Mysyrowicz A 1996 *Opt. Lett.* **21** 62–4  
Braun A, Korn G, Liu X, Du D, Squier J and Mourou G 1995 *Opt. Lett.* **20** 73–5  
Mlejnek M, Kolesik M, Moloney J V and Wright E M 1999 *Phys. Rev. Lett.* **83** 2938–41
- [22] Brodeur A, Chien C Y, Ilkov F A, Chin S L, Kosareva O G and Kandidov V P 1997 *Opt. Lett.* **22** 304–6
- [23] Mlejnek M, Wright E M and Moloney J V 1998 *Opt. Lett.* **23** 382–4
- [24] Liu W, Gravel J F, Théberge F, Becker A and Chin S L 2005 *Appl. Phys. B* **80** 857–60  
Liu W, Théberge F, Arevalo E, Gravel J F, Becker A and Chin S L 2005 *Opt. Lett.* **30** 2602–4
- [25] Brabec T and Krausz F 1997 *Phys. Rev. Lett.* **78** 3282–5
- [26] Brabec T and Krausz F 2000 *Rev. Mod. Phys.* **72** 545–91
- [27] Aközbebek N, Scalora M, Bowden C M and Chin S L 2001 *Opt. Commun.* **191** 353–62
- [28] Becker A, Plaja L, Moreno P, Nurhuda M and Faisal F H M 2001 *Phys. Rev. A* **64** 023408
- [29] Nibbering E T J, Grillon G, Francois M A, Prade B S and Mysyrowicz A 1997 *J. Opt. Soc. Am. B* **14** 650–60
- [30] Zheltikov A M 2005 *Phys. Rev. A* **72** 043812

- [31] Couairon A 2003 *Appl. Phys. B* **76** 789–92
- [32] Lange H R, Grillon G, Ripoche J F, Franco M A, Lamouroux B, Prade B S, Mysyrowicz A, Nibbering E T J and Chiron A 1998 *Opt. Lett.* **23** 120–2
- [33] Liu W, Luo Q, Théberge F, Xu H L, Hosseini S A, Sarifi S M and Chin S L 2006 *Appl. Phys. B* **82** 373–6
- [34] Couairon A, Franco M, Mysyrowicz A, Biegert J and Keller U 2005 *Opt. Lett.* **30** 2657–9
- [35] Couairon A, Biegert J, Hauri C P, Kornelis W, Helbing F W, Keller U and Mysyrowicz A 2006 *J. Mod. Opt.* **53** 75–85
- [36] Koprinkov I P, Suda A, Wang P Q and Midorikawa K 2000 *Phys. Rev. Lett.* **84** 3847–50
- [37] Li R, Chen X, Liu J, Leng Y, Zhu Y, Ge X, Lu H, Lin L and Xu Z 2005 *SPIE Proc.* **5708** 102–11
- [38] Trushin S A, Fuß W, Kosma K and Schmid W E 2006 *Appl. Phys. B* (doi 10.1007/S00340)